Journal of Energy Challenges and Mechanics
http://www.nscj.co.uk/JECM/
ISSN 2056-9386
Volume 1 (2014) issue 1, article 6

Drilling Mud Loss in a Natural Fracture - A PKN Fracture Geometry Model Based Analysis

天然裂缝中钻井液的漏失-基于PKN裂缝几何模型的分析

Yixuan Sun（孙义轩）, Haiying Huang*（黄海鹰）

School of Civil and Environmental Engineering, Georgia Institute of Technology, Atlanta, GA 30332, USA

haiying.huang@ce.gatech.edu

Accepted for publication on 5th August 2014

Abstract - **A mathematical model is formulated in this work to determine the drilling mud loss in a natural fracture intersected by a wellbore. The formulation is based on a PKN fracture geometry model, assuming the natural fracture intersects the wellbore with the fracture plane more or less parallel to the wellbore axis. The drilling mud is treated as a single-phase fluid. The rheology of the drilling mud is assumed to be non-Newtonian of Herschel-Buckley type. The reservoir formation is assumed to be permeable with the leak off following Carter's model. Fluid flow along the fracture is considered as one-dimensional lubrication flow. Deformation of the fracture is governed by local elasticity and the wellbore pressure and the pore pressure in the reservoir are assumed to be constant. The problem defined above is solved numerically using an explicit moving mesh algorithm. Effects of the yield stress and the overbalance pressure on the drilling mud loss are evaluated.**

Keywords – **drilling mud loss, PKN fracture model, natural fracture**

摘要 **－ 天然裂缝性地层容易出现严重的井漏。在过平衡钻井时，大量钻井液的漏失不仅影响钻井操作，而且还会对随后的完井及油藏的生产产生不良影响。为了能够合理地采取措施减少井漏，我们迫切需要对钻井液在天然裂缝的漏失进行定量预测。本文将建立一个基于PKN裂缝几何形状的数学模型对天然裂缝中钻井液的漏失进行模拟计算。我们假设天然裂缝与井筒相交，裂缝平面大致平行于井孔轴。钻井液将被视为单相流体。钻井液的流变特性采用非牛顿流体的赫谢尔-巴克利模型。钻井液在地层中的渗透将由卡特模型来描述,在裂隙中的流动是一维的，可以由流体润滑方程来描述。地层的变形假设是局部弹性的。井中压力和油藏孔隙压力假设是常值。 显式移动网格算法将被用于求解上述问题。本文将对流变参数和过平衡压力对钻井液漏失的影响进行评估。**

关键词 **－ 钻井液漏失, PKN裂缝模型, 天然裂缝**

I. INTRODUCTION

Naturally fractured reservoirs are prone to severe circulation losses. In overbalance drilling, since the wellbore pressure is larger than the reservoir pore pressure, large volume loss of the drilling mud in fractured formations could be a significant problem not only in the drilling operation but also during subsequent well completion and reservoir production. Quantitative prediction of the drilling mud loss is therefore critically needed for the control of lost circulation. In general, drilling mud may be treated as a single-phase incompressible fluid displaying non-Newtonian rheological characteristics such as yield stress and shear thinning. The yield stress is the most critical rheological element responsible for the eventual cessation of mud invasion. Loss of the drilling mud in the natural fracture is driven by the pressure drop between the wellbore and the reservoir. The pressure gradient near the wellbore is the largest at the onset of drilling mud invasion and decreases as the mud flows further into the fracture. For a yield stress fluid, when the pressure gradient falls below a threshold, mud invasion ceases and the fracture can be considered sealed. The Herschel-Buckley model with a yield stress and power law for shear thinning has been considered an accurate description for the drilling mud rheology, especially in the low shear rate range [1].

Drilling mud loss in a natural fracture has been previously modeled in the literature assuming radial flow through two parallel disks with or without the consideration of reservoir deformation, e.g. [2][3]. The assumption of radial flow is most applicable when the natural fracture is nearly perpendicular to the wellbore axis.

In this work, a mathematical model is formulated to determine the drilling mud loss for the scenario when the natural fracture intersects the wellbore with the fracture plane aligned more or less parallel to the wellbore axis. The natural fracture is initially closed. Fluid flow inside the fracture is coupled with the mechanical deformation of the permeable reservoir. The fracture opening developed as a result of mud invasion is assumed to be elliptical with a constant height, following the Perkins-Kern-Nordgen (PKN) geometry model [4][5].

An explicit moving mesh algorithm modified from those for solving the PKN hydraulic fracturing model for power law [6] and piecewise power law rheology [7] is employed in this study. The mathematical formulation and the numerical implementation are first presented. Effects of the yield stress

and the overbalance pressure on the drilling mud loss are then analyzed.

II. MATHEMATICAL FORMULATION

Schematic of a PKN geometry model of length L and height H is shown in Fig. 1. A key assumption in the PKN hydraulic fracture model is that the elastic response of the rock is local, namely, the opening of the hydraulic fracture at a given position x depends on the local overpressure only, but not on the pressure everywhere else inside the fracture, i.e.,

$$p = \frac{w}{M_c} \tag{1}$$

Eq. (1) states that the average fracture width w of a cross section is related to the net local pressure p through the fracture compliance $M_c = \pi(1-\nu)H/4G$, where G and ν are the shear modulus and the Poisson's ratio of the rock, respectively. The net pressure p, i.e., the overpressure above the reservoir stress, is assumed to vary only along the $x-$axis, namely, the direction of fracture propagation, and is uniform at a given cross section. The average width is defined according to $w = A/H$, where A is the cross sectional area. For an elliptical cross section, if the width at the mid-height is w_0 (see Fig. 1), $w = \pi w_0/4$. The local elasticity assumption implies each cross section is deforming independently under the condition of plane strain, which is most applicable when the fracture length is much larger than the fracture height and the fracture width is much smaller than the height [8]. The local elasticity assumption relieves us of solving the integral form pressure-width relation required in other hydraulic fracture geometry models such as the KGD [9][10] and the penny-shaped fracture models [11]. The PKN hydraulic fracture model therefore offers unique simplicity that allows incorporation of complex fluid rheology.

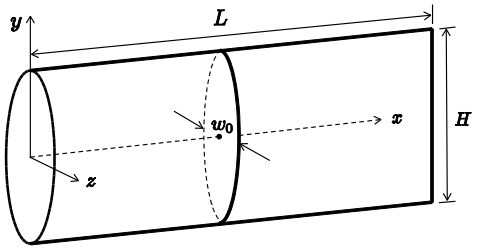

Fig. 1, A PKN fracture of length L and height H; at a given cross section, the fracture width at the mid-height is denoted as w_0.

We may assume that fluid flow along the fracture is one-dimensional. Consequently, the local continuity equation can be written as,

$$\frac{\partial q_x}{\partial x} + \frac{\partial w}{\partial t} + u = 0 \tag{2}$$

where q_x is the flow rate per unit height of a cross section; t is the elapsed time from the onset of drilling mud invasion and u is the fluid leak off velocity from the fracture faces. For a relatively low permeability formation, fluid leak off may be assumed to be one-dimensional obeying Carter's leak off model,

$$u = \frac{2C_L}{\sqrt{t - t_a(x)}} \tag{3}$$

where C_L is the leak off coefficient and $t_a(x)$ is the fracture tip arrival time at location x. Carter's leak off model, Eq. (3), relates the leak off velocity u to the time of exposure for a given position. The velocity u accounts for the leak off from both sides of the fracture faces.

Fluid rheology is only involved in the equation of balance of fluid momentum for the PKN hydraulic fracture model. With the assumption of one dimensional lubrication flow, the equation of balance of momentum can be approximated by integrating the Poiseuille slot flow solution over the height of the elliptical cross section. The slot flow solution for a Herschel-Buckley fluid therefore needs to be derived first.

For a Herschel-Buckley fluid, the relationship between the shear stress and the shear strain rate can be expressed as,

$$\tau = \begin{cases} \tau_0 & \dot{\gamma} = 0 \\ \tau_0 + K\dot{\gamma}^n & \dot{\gamma} > 0 \end{cases} \tag{4}$$

where τ_0, K and n are the yield stress, the consistency parameter and the power index. Fluid flow occurs only if the shear stress τ exceeds the yield stress τ_0.

After combining the rheology model with the equilibrium equation, the geometrical equation, and the no-slip condition at the slot walls, the steady state velocity profile for slot flow can be readily obtained,

$$V_x = \begin{cases} \dfrac{bn\left(\dfrac{\bar{p}b}{K}\right)^{\frac{1}{n}}}{1+n}\left[(1-s_*)^{1+\frac{1}{n}} - (|s|-s_*)^{1+\frac{1}{n}}\right] & |s| > s_* \\ \dfrac{bn\left(\dfrac{\bar{p}b}{K}\right)^{\frac{1}{n}}}{1+n}(1-s_*)^{1+\frac{1}{n}} & |s| \le s_* \end{cases} \tag{5}$$

where V_x is the fluid flow velocity in the flow direction; b is the half width of the slot; $s = y/b$ is the scaled coordinate $(-1 \le s \le 1)$ in the slot width direction and $\bar{p} = |dp/dx|$ is the magnitude of the pressure gradient in the fluid flow direction. Due to the existence of the yield stress, within the region of $|s| \le s_*$, the velocity is constant and fluid flows in a plug form. The critical pressure gradient to initiate fluid flow is $\bar{p}_c = \tau_0/b$ and the half width s_* of the plug flow region can be determined from $s_* = \tau_0 b/\bar{p}$.

The total flow rate Q_x^s at a given pressure gradient $\bar{p}$ for slot flow can be obtained by integrating the velocity across the slot width,

$$Q_x^s = \frac{2b^{2+\frac{1}{n}}\left(\dfrac{\bar{p}}{K}\right)^{\frac{1}{n}}}{1+\dfrac{1}{n}}(1-s_*)^{1+\frac{1}{n}}\left(\frac{n+1+s_*}{2n+1}\right) \tag{6}$$

Fig. 2 shows the variation of the velocity profiles with respect to the applied pressure gradient $\bar{p} = 0.05, 0.1$ and 0.2 MPa/m for the following rheological parameters: $\tau_0 = 10$ Pa, $n = 0.7$, and $K = 0.3$ Pa·s^n. As can be seen from Fig. 2, the plug zone size reduces as the pressure gradient $\bar{p}$ increases. The pressure gradient and the flow rate relationship as shown

in Fig. 3 indicates that the flow rate is zero before the yield stress is overcome by the pressure gradient along the slot.

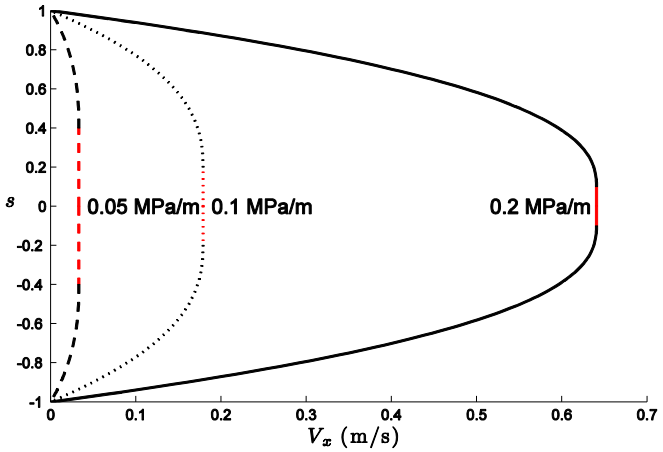

Fig. 2, Velocity profiles under different pressure gradients; the red lines denote the plug flow zones.

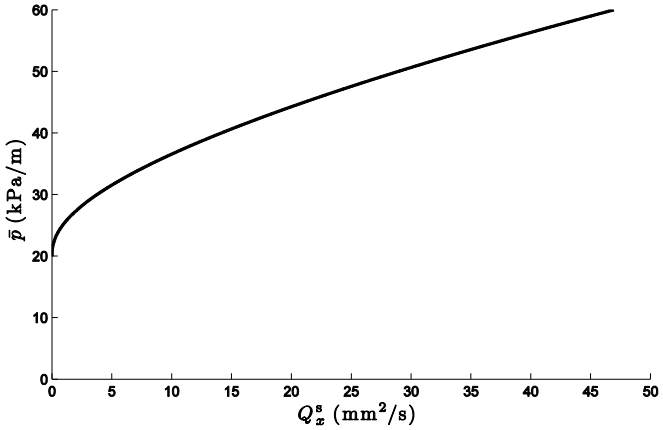

Fig. 3, Variation of the pressure gradient with respect to the total flow rate for slot flow.

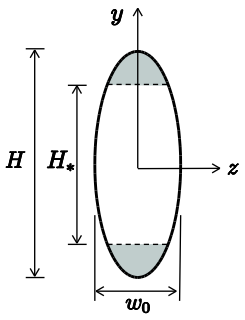

Fig. 4, A PKN model cross section for a Herschel-Buckley fluid.

With the assumption of one-dimensional lubrication flow inside the fracture, the existence of the yield stress is manifested through the stagnation zones near the two ends of the fracture cross section, as shown in the shaded areas in Fig. 4. The ratio between the height H_* of the moving fluid region and the total height H can be determined from,

$$\frac{H_*}{H} = \sqrt{1 - \left(\frac{2\tau_0}{\bar{p} w_0}\right)^2} \tag{7}$$

At a given height position, the local flow rate Q_x can be obtained based on the slot flow solution, Eq. (6),

$$Q_x = \begin{cases} \dfrac{2\left(\frac{w_y}{2}\right)^{2+\frac{1}{n}}\left(\frac{\bar{p}}{K}\right)^{\frac{1}{n}}}{1+\frac{1}{n}}(1-s_*)^{1+\frac{1}{n}}\left(\dfrac{n+1+s_*}{2n+1}\right) & |y| < \dfrac{H_*}{2} \\ 0 & \dfrac{H_*}{2} \le |y| < \dfrac{H}{2} \end{cases} \tag{8}$$

where w_y is the fracture width at a given height y, $w_y = w_0\sqrt{1-(2y/H)^2}$.

The balance of momentum equation relating the total flow rate or the mud loss rate per unit height q_x to the local pressure gradient $\bar{p}$ can be obtained by integrating Eq. (8) over the fracture height,

$$q_x = \frac{C_1}{\bar{p}^2}\left[M_1 - \frac{1}{3}\left(\frac{H_*}{H}\right)^2 M_2\right]\left[\left(\frac{w_0}{2}\right)\bar{p} - \tau_0\right]^{1+1/n}\left[\left(1+\frac{1}{n}\right)\left(\frac{w_0}{2}\right)\bar{p} + \tau_0\right] \tag{9}$$

where,

$$\begin{aligned} C_1 &= \frac{2}{\left(1+\frac{1}{n}\right)\left(2+\frac{1}{n}\right)K^{\frac{1}{n}}}\left(\frac{H_*}{H}\right) \\ M_1 &= {}_2F_1\left[\frac{1}{2}, -\frac{1}{2n}, \frac{3}{2}, \left(\frac{H_*}{H}\right)^2\right] \\ M_2 &= {}_2F_1\left[\frac{3}{2}, -\frac{1}{2n}, \frac{5}{2}, \left(\frac{H_*}{H}\right)^2\right] \end{aligned} \tag{10}$$

where ${}_2F_1[\ \ ]$ denotes the hypergeometric function.

To complete the formulation, boundary conditions both at the wellbore and at the fracture tip need to be supplied. We may assume that the wellbore overpressure P_{in} is constant and the initial reservoir pore pressure and the reservoir stress are both constant, which serve only as references. In addition, no flow condition can be imposed at the fracture tip $x = L$, i.e.,

$$\begin{aligned} p &= P_{\text{in}} \quad \text{at } x = 0 \\ w = 0,\ q_x &= 0 \quad \text{at } x = L \end{aligned} \tag{11}$$

III. Numerical Implementation

The system of governing equations, Eqs. (1) – (3) and Eq. (9), is first transformed by introducing a moving coordinate $\theta = x/L(t)$, $\theta \in [0,1]$. An equation for the fracture width can be obtained as follows,

$$\dot{w}_0 = \frac{\theta \dot{L}}{L}\frac{\partial w_0}{\partial \theta} + c_w \frac{\partial^2 w_0}{\partial \theta^2} + c_s\left(\frac{\partial w_0}{\partial \theta}\right)^2 \tag{12}$$

where $\dot{(\ )} = d(\ )/dt$ is the material time derivative and c_w and c_s are functions of the material parameters and the fracture width w_0 and the gradient $\partial w_0/\partial\theta$. For brevity, expressions for c_w and c_s are omitted here.

Such a "diffusion-type" of equation for the width w_0 can be solved by using an explicit finite-difference scheme [6]. After

discretizing the fracture length into N nodes, at a given time step, say, $t = t^{k+1}$, the critical time step to ensure numerical stability can be computed from,

$$\Delta t_c^{k+1} = \min\left[\frac{\Delta\theta_i^2}{2(c_w)_i^k}\right];\ \ i = 1, \cdots, N-1 \qquad (13)$$

Here the nodal number is denoted by the subscript i and the time step is denoted by the superscript k for simplicity, e.g., $(c_w)_i^k = c_w(\theta_i, t^k)$. In the time-stepping algorithm, after knowing all the nodal quantities in the previous time step, a critical time step is first chosen. The fracture width w, the net fluid pressure p in the fracture, the local flow rate q_x, the leak off velocity u, and the fracture length L, are computed sequentially.

Since the numerical scheme is explicit, an initial guess is required to start the calculation. The analytical solution for the PKN model in an impermeable formation with a power law fluid [12] is used as the initial guess for the fracture length, width and the flow rate at an arbitrarily small starting time. As shown in [7], with the proper choice of the critical time step, the numerical scheme is robust and the solutions are not sensitive to the initial guesses obtained from different rheology.

IV. Numerical Results

Effects of the yield stress and the overbalance pressure on the drilling mud loss behaviors are investigated using the set of input parameters as listed in Table I.

TABLE I, INPUT PARAMETERS FOR THE SIMULATION CASES

Consistence parameter, K	0.3 Pa·s$^{0.7}$
Power law index, n	0.7
Poisson's ratio, ν	0.2
Shear modulus, G	10 GPa
Fracture height, H	10 m
Leak-off coefficient, C_L	6.3×10^{-5} m/s$^{1/2}$

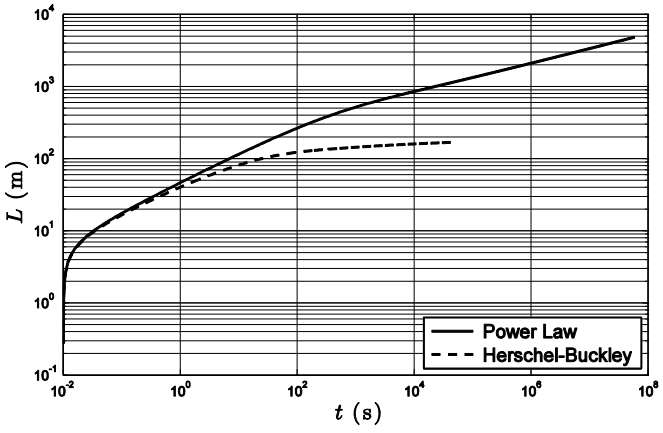

Fig. 5, Fracture length as a function of time from the simulation cases with a power law fluid and a Herschel-Buckley fluid ($\tau_0 = 100$ Pa) with an overpressure $P_{\text{in}} = 10$ MPa.

Variations of the fracture length or the mud invasion length with time for a power law fluid and a Herschel-Buckley fluid are compared in Fig. 5. The two cases have the same power law parameters and the wellbore overpressure is $P_{\text{in}} = 10$ MPa. The yield stress for the Herschel-Buckley fluid is $\tau_0 = 100$ Pa. The Herschel-Buckley solution coincides with the power-law solution at early time, but gradually deviates from the power law solution at late time. This means that fluid flow is governed by the high shear rate rheology at early time, but by the low shear rate rheology at late time. Eventually, the Herschel-Buckley solution reaches a plateau, indicating that the fracture is no longer propagating. In other words, there is no further mud invasion into the fracture. Meanwhile, for the power law case, the absence of the yield stress results in continuous fracture growth and the fracture cannot be sealed.

Evolution of the fracture half-width is plotted against the fracture length at different times for a case with $\tau_0 = 10$ Pa and $P_{\text{in}} = 5$ MPa. Since the fracture width at the inlet is governed by the inlet pressure and the fracture compliance, it remains constant as the fracture propagates. Meanwhile, the gradient of the fracture width, and thus the pressure gradient, decreases and the rate of increase in the fracture length or the mud invasion length decreases with time.

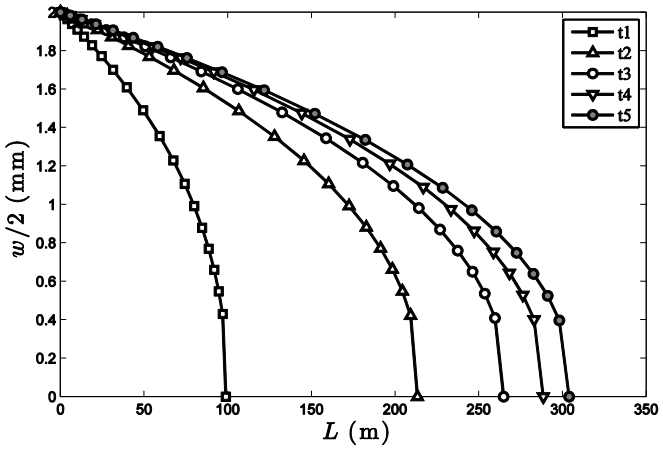

Fig. 6, Evolution of the fracture width profile with time with $P_{\text{in}} = 5$ MPa and $\tau_0 = 10$ Pa, and $t_1 = 506.6$ s, $t_2 = 8.558e4$ s, $t_3 = 4.709e5$ s, $t_4 = 9.949e5$ s, $t_5 = 1.608e6$ s.

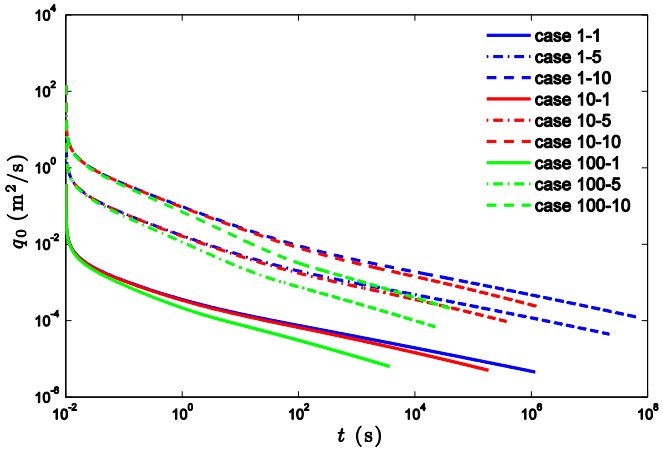

Fig. 7, Evolution of the inlet flow rate per unit height q_0 with time t; the case numbers refer to the yield stress in Pa and the overpressure in MPa; namely, case 10-1 is a test case with $\tau_0 = 10$ Pa and $P_{\text{in}} = 1$ MPa.

A series of simulations are conducted by varying the yield stress and the inlet overpressure, $\tau_0 = 1$, 10, 100 Pa and

$P_{in} = 1, 5, 10$ MPa, to investigate their influences on the mud loss rate at the inlet q_0 (per unit height) and the fracturing efficiency η. The fracturing efficiency is defined according to $\eta = (V - V_\ell)/V$, where V is the total volume of mud loss and V_ℓ is the volume of fluid leaked into the formation. The efficiency measures the percent of fluid volume stored inside the fracture. Though, in the range of parameters explored, the drilling mud loss behavior is predominantly affected by the prescribed inlet pressure, increasing the yield stress to $\tau_0 = 100$ Pa has a considerable effect on the mud loss rate. As can be seen from Fig. 7, the mud loss rate for $\tau_0 = 100$ Pa and $P_{in} = 10$ MPa indeed becomes smaller than that in the cases with $\tau_0 = 1$ and 10 Pa and $P_{in} = 5$ MPa at late time.

As shown in Fig. 8, the fracturing efficiency decreases with time, suggesting that at the early stage, a higher percentage of the drill mud loss is in opening up the natural fracture. Matrix leak off becomes relatively important only at the later stage.

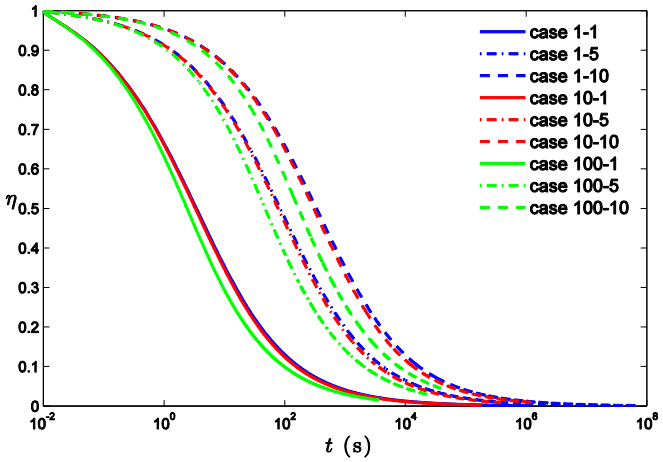

Fig. 8, Variation of the fracturing efficiency η with time t; the case numbers refer to the yield stress in Pa and the overpressure in MPa; namely, case 10-1 is a test case with $\tau_0 = 1$ Pa and $P_{in} = 1$ MPa.

V. Conclusion

In this paper, a mathematical model for predicting drilling mud loss in a natural fracture is developed based on the classical PKN hydraulic fracture geometry model. Rheology of the drilling mud is assumed to be non-Newtonian of Herschel-Buckley type. The numerical scheme using an explicit moving mesh algorithm provides a robust tool that allows not only systematic investigation of the effects of the formation and the fluid characteristics on the drilling mud loss, but also improvement in the fluid design to control lost circulation.

Acknowledgements

Support from the National Science Foundation through grant NSF/CMMI-1055882 is gratefully acknowledged.

References

[1] T. Hemphill, W. Campos, and A. Pilehvari. "Yield-power law model more accurately predicts mud rheology," *Oil and Gas Journal*, **91**, pp. 1993.

[2] A. Lavrov. "Modeling flow of a biviscous fluid from borehole into rock fracture," *Journal of Applied Mechanics*, **73**, pp. 171-173, 2006.

[3] R. Majidi, S. Miska, R. Ahmed, M. Yu, and L. Thompson. "Radial flow of yield-power-law fluids: Numerical analysis, experimental study and the application for drilling fluid losses in fractured formations," *Journal of Petroleum Science and Engineering*, **70**, pp. 334-343, 2010.

[4] T. Perkins and L. Kern. "Widths of hydraulic fractures," *Journal of Petroleum Technology*, **13**, pp. 937-949, 1961.

[5] R. Nordgren. "Propagation of a vertical hydraulic fracture," *SPE Journal*, **12**, pp. 306-314, 1972.

[6] E. Detournay, A. H-D. Cheng, and J. McLennan, "A poroelastic PKN hydraulic fracture model based on an explicit moving mesh algorithm," *Journal of Energy Resources Technology*, **112**, pp. 224-230, 1990.

[7] H. Huang and J. Desroches. "A PKN hydraulic fracturing model with piecewise fluid rheology," *Gulf Rocks 2004, Proceedings of the 6th North America Rock Mechanics Symposium (NARMS)*, Houston, Texas, United States, June 5--9, 2004.

[8] J. Geertsma and R. Haafkens. "A comparison of the theories for predicting width and extent of vertical hydraulically induced fractures," *Journal of Energy Resources Technology*, **101**, pp. 8-19, 1979.

[9] S. Khristianovic and Y. Zheltov. "Formation of vertical fractures by means of highly viscous fluids," Vol. 2, *Proceedings of the 4th World Petroleum Congress*, Rome, Italy, June 6--15, 1955.

[10] J. Geertsma and F. De Klerk. "A rapid method of predicting width and extent of hydraulically induced fractures," *Journal of Petroleum Technology*, **21**, pp. 1571-1581, 1969.

[11] H. Abe, T. Mura and L. Keer. "Growth rate of a penny-shaped crack in hydraulic fracturing of rocks," *Journal of Geophysical Research*, **81**, pp. 5335-5340, 1976.

[12] K. Nolte and M. Smith, "Interpretation of fracturing pressures," *Journal of Petroleum Technology*, **33**, pp. 1767-1775, 1981.